

Structural Verification and Reinforcement Calculation of the Cylindrical Shaft in Kokhav Hayarden Power Plant

Hua LI^a, Feng MA^a and An LIU^{a,1}

^a PowerChina Huadong Engineering Corporation Limited, Hangzhou, China

Abstract. Special attention deserves the provision of reinforcement to prevent cracking problems associated with the phenomena of shrinkage and temperature associated with the generation of cement hydration heat during concrete setting, which can induce significant deformations and stresses due to the volume change associated with the concrete mass temperature increase. The cylindrical shaft in power plant is a massive underground structure and of great importance to the security during construction. In this paper, the minimum reinforcement as initial design is adopted, then checks are performed for verifying operational and seismic conditions. Using uniform distribution of vertical reinforcement, the initial distribution of the longitudinal reinforcement of the LSS cylindrical shaft was calculated to verify its stability. This paper mainly presents the results of structure calculation based on an update of the geotechnical parameters resulting from the LSS monitoring layout and load combinations, with special attention to the seismic response and its interaction with the surrounding rock and the amplifying effects on the Control Room.

Keywords. Power plant, cylindrical shaft, structure verification

1. Introduction

The Lower Surge Shaft of Kokhav Hayarden Pumped Storage Plant (abbreviated to LSS in the following) is hereafter examined concerning structural behaviour [1]. The cylindrical shaft, between the EL.-285.16 m and EL.-187.30 m, consists of a cylindrical structure of 16.60-17.60 m in diameter and 97.86 m in length, using three sections with lining thicknesses of 80, 110, and 130 cm. Because it is a massive concrete structure, special attention deserves the provision of reinforcement to prevent cracking problems associated with the phenomena of shrinkage and temperature associated with the generation of cement hydration heat during concrete setting, which can induce significant deformations and stresses due to the volume change associated with the concrete mass temperature increase [2,3].

For elements subjected to environmental exposure conditions or required to be liquid-tight, when joint is not provided and use reinforcement $f_{yk} > 400$ MPa, the area of shrinkage and temperature reinforcement shall provide at least 0.005 to the gross concrete area. This reinforcement may be reduced to 50 percent on supported soil

¹ An LIU, Corresponding Author, PowerChina Huadong Engineering Corporation Limited, China; Email: liu_a2@hdec.com

elements [4,5]. In this case, since the LSS cylindrical shaft is a massive underground structure, the ACI 350R-01 criterion is adopted to define the minimum reinforcement as initial design, then, checks are performed for verifying operational and seismic conditions [6,7]. Using a uniform distribution of vertical reinforcement (694 ϕ -@200), table 1 shows the initial distribution of the longitudinal reinforcement of the LSS cylindrical shaft.

Table 1. Distribution of the longitudinal reinforcement.

| Section | Lining Thickness (cm) | Ac (m ²) | As _{min} (cm ²)=0.25% \times Ac | As (cm ²) | ρ_s = As/Ac |
|---------|-----------------------|----------------------|--|------------------------|------------------|
| I | 130 | 109.80 | 2745 | 694 ϕ 25@200=3406 | 0.31% |
| II | 110 | 98.80 | 2470 | 694 ϕ 22@200=2637 | 0.27% |
| III | 80 | 82.90 | 2072 | 694 ϕ 20@200=2180 | 0.26% |

2. Simulation of Bending Strength

The evaluation of the moment-curvature diagrams of the three cross-sections analyzed for different axial compression loads corresponding to the weight of the concrete structure above the elevation considered. As an example, figure 1 shows the vertical reinforcement distribution for section III with 80 cm lining thickness. Figure 2 shows the moment-curvature diagram around the Y-Y axis (vertical) for a positive moment (compression to the right) and a negative moment (compression to the left). The section is symmetrical to the X-axis. In particular, the results are presented for an axial load of 94150 KN corresponding to EL.-212.60m.

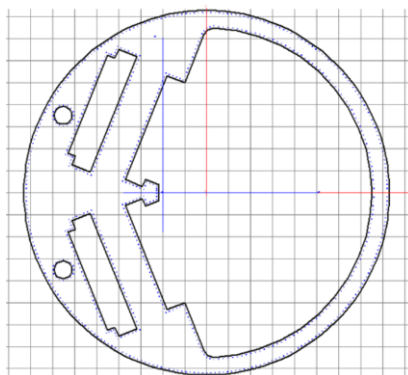


Figure 1. Effective section of the LSS cylindrical shaft.

In each interaction diagram, three characteristic points (characteristic moments) corresponding to the moment of cracking (M_{cr}), the moment yielding (M_y), and the ultimate moment (M_u) are featured.

Table 2 summarizes the results obtained for seven types of sections/elevations considered with the minimum reinforcement cited in table 1. It highlights the elevation of the section, the lining thickness, the average axial load, and the moments associated with the characteristic points. In particular, for the moments around the Y-axis, the upper value corresponds to the negative moment and the lower value to the positive moment.

Table 2. Characteristic moments for section types.

| Elevation (m) | Section | Thickness (cm) | Pmax (KN) | Mcr (KN-m) | My (KN-m) | Mu (KN-m) |
|---------------|---------|----------------|-----------|------------|-----------|-----------|
| -187.30 | III | 80 | 42765 | 106975 | 769360 | 1090990 |
| -212.60 | III | 80 | 94150 | 241065 | 1106100 | 1475270 |
| -220.10 | II | 110 | 131670 | 320570 | 1481055 | 1961370 |
| -246.83 | III | 110 | 169710 | 391640 | 1573085 | 1996260 |
| -259.50 | II | 110 | 200380 | 561880 | 1950660 | 2454500 |
| -281.40 | II | 110 | 253390 | 644395 | 2256230 | 2814255 |
| -285.16 | I | 130 | 263500 | 752590 | 2175260 | 2875045 |

Figure 2 shows a comparison of the bending moment Demand-Capacity along the shaft through the superimposing of the moment envelopes (Demand) obtained from the analysis with the FLAC model, with the sections characteristic moments (Capacity) for MDE in direction Y ad X respectively. In particular, the green segmented line represents the moment of cracking (Mcr), the yellow segmented line represents the yielding moment (My) and the red segmented line represents the ultimate moment (Mu). In these figures, the acting moment is directly compared with the resistant moment around the main directions of the section.

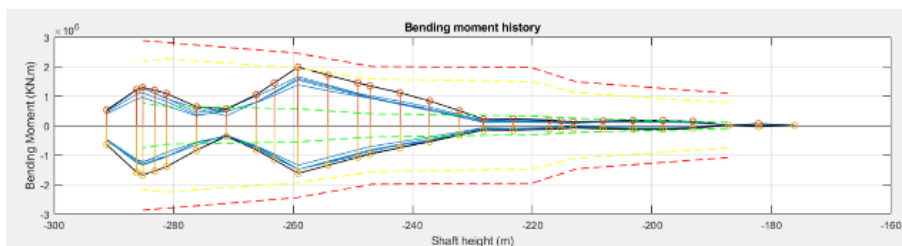


Figure 2. Bending moment Demand-Capacity comparison along the shaft.

From the previous figure, it is concluded that for the definition of longitudinal reinforcement preliminarily adopted. For the Maximum Design Earthquake MDE, the demands of bending moments are kept below the resistance of the section - ultimate moment Mu (red segmented line). For the Operational Basis Earthquake OBE, the demands of bending moments remain below the elastic limit of the section - yielding moment My (yellow segmented line), and even in most of the shaft, it is maintained by below the moment of cracking of the section-moment of cracking Mcr (green segmented line). It is also possible to verify that the maximum values obtained for the particular study case OBE3 remain below the maximum value determined for MDE factored by (PGA_{OBE} / PG_{AMDE}), thereby confirming the hypothesis that the values for OBE can be conservatively obtained scaling the results obtained for the MDEs through a factor proportional to the ratio of the Peak Ground Acceleration PGA_{OBE} / PG_{AMDE} = 0.25g / 0.44g = 0.568.

Figures 3 and 4 show a comparison of the bending moment Demand-Capacity along the shaft through the superimposing of the moment (Demand) obtained from the analysis with the sections characteristic moments (Capacity) for OBE3 in direction X ad Y respectively. In particular, the green segmented line represents the moment of cracking (M_{cr}), the yellow segmented line represents the yielding moment (M_y) and the red segmented line represents the ultimate moment (M_u). In these figures, the acting moment is directly compared with the resistant moment around the the main directions of the section.

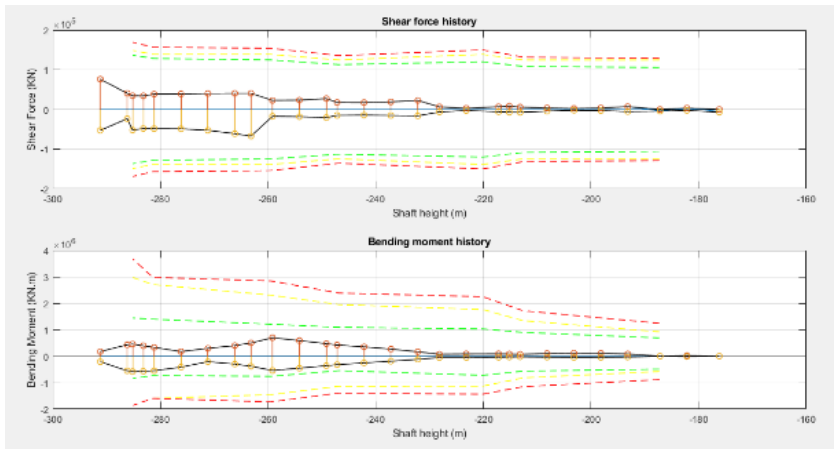


Figure 3. Bending moment Demand-Capacity comparison along the shaft.

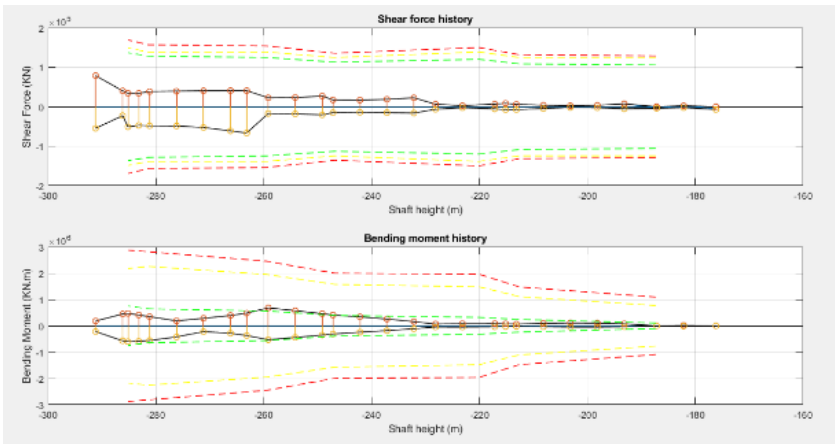


Figure 4. Bending moment Demand-Capacity comparison along the shaft.

From the previous figures, it is concluded that for the definition of longitudinal reinforcement preliminarily adopted;

For the Maximum Design Earthquake MDE (associated with an average return period $T = 2475$ years), the demands of bending moments are kept below the resistance of the section - ultimate moment M_u (red segmented line).

For the Operational Basis Earthquake OBE (associated with an average return period $T = 475$ years), the demands of bending moments remain below the elastic limit

of the section - yielding moment M_y (yellow segmented line), and even in most of the shaft, it is maintained by below the moment of cracking of the section - moment of cracking M_{cr} (green segmented line).

It is also possible to verify that the maximum values obtained for the particular study case OBE3 remain below the maximum value determined for MDE factored by (PGA_{OBE} / PGAMDE), thereby confirming the hypothesis that the values for OBE can be conservatively obtained scaling the results obtained for the MDEs through a factor proportional to the ratio of the Peak Ground Acceleration $PGA_{OBE}/ PGAMDE = 0.25g / 0.44g = 0.568$

3. Check Design with the Moment Combinations

According to the results, the amounts of vertical reinforcement have been rectified in accordance with the finally adopted reinforcement. The evaluation of the shear strength of the section is more difficult. As a simplification, a circular hollow cross-section with a thickness equal to the lining thickness is conservatively adopted for evaluation purposes, neglecting the contribution of the extra concrete in the interior of the cross-section. The proposed model evaluates the shear strength as the summation of the contributions, one due to concrete shear resisting mechanisms (V_c), and the other due to transverse steel reinforcement (V_s). Using the preliminary longitudinal reinforcement defined in table 1, the associated axial loads for each elevation defined in table 3, the angle between the concrete compression strut and the beam axis perpendicular to the shear force $\theta=30^\circ$, and preliminarily assume a circumferential reinforcement consisting of $\phi 25@200$ on every hollow circular cross-section faces ($A_{st}=5 \times 4.91 \text{ cm}^2$).

Table 3. Shear force resistance.

| Elevation (m) | Eurocode $V_r(\text{KN})$ | Priesley et al. $V_r(\text{KN})$ | Moehle et al. $V_r(\text{KN})$ |
|---------------|------------------------------|-------------------------------------|-----------------------------------|
| -187.3 | 105589 | 124496 | 128754 |
| -212.6 | 108543 | 124496 | 131671 |
| -220.1 | 120004 | 138643 | 149869 |
| -246.83 | 122886 | 138643 | 152548 |
| -259.5 | 124647 | 138643 | 153969 |
| -281.4 | 128229 | 138643 | 156923 |
| -285.16 | 136732 | 148948 | 169064 |

Figure 5 shows a comparison of the shear force Demand-Capacity along the shaft through the superimposing of the shear (demand) obtained from the analysis with the FLAC model, with the shear strength (capacity) for MDE in direction Y and X respectively. In particular, the green segmented line represents the shear strength Eurocode 2 approach.

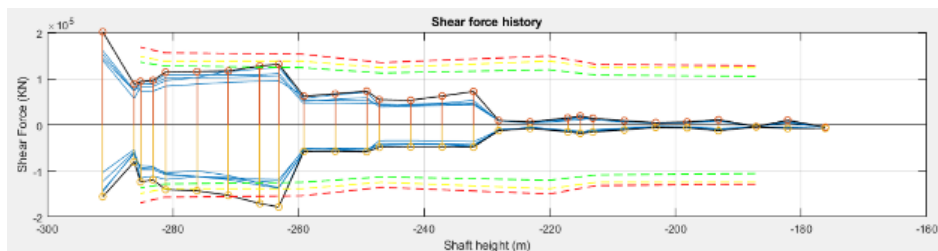


Figure 5. Shear force Demand-Capacity comparison along the shaft.

4. Conclusion

This paper mainly presents the results of structure calculation based on an update of the geotechnical parameters resulting from the LSS monitoring layout and load combinations. For the definition of circumferential reinforcement preliminarily adopted, for the Maximum Design Earthquake MDE, the demands of shear force are kept below the shear resistance of the section- V_u , regardless of the evaluation approach used, except in the shaft sector below elevations EL.-260m, where the transverse reinforcement density must be increased.

Competing Interests

The authors declare that they have no known competing financial interests or personal relationships that could have appeared to influence the work reported in this paper.

References

- [1] Cobas C. NMR signal processing, prediction, and structure verification with machine learning techniques. *Magnetic Resonance in Chemistry*, 2020; 58(6): 512-519.
- [2] Ding XL, Wang YC, Wang YB, et al. A review of structures, verification, and calibration technologies of space robotic systems for on-orbit servicing *Science China Technological Sciences*. 2021; 64(3): 462-480.
- [3] Kuzina ES, Rimshin VI. Calculation method analysis for structure strengthening with external reinforcement. *IOP Conference Series: Materials Science and Engineering*. IOP Publishing, 2020; 753(2): 022004.
- [4] Telichenko V, Rimshin V, Kuzina E. Methods for calculating the reinforcement of concrete slabs with carbon composite materials based on the finite element model. *MATEC Web of Conferences*. EDP Sciences. 2018; 251: 04061.
- [5] Chen P, Zhou X, Zheng W, et al. Influence of high sustained loads and longitudinal reinforcement on long-term deformation of reinforced concrete beams. *Journal of Building Engineering*. 2020; 30: 101241.
- [6] Sabzi J, Esfahani MR, Ozbakkaloglu T, et al. Effect of concrete strength and longitudinal reinforcement arrangement on the performance of reinforced concrete beams strengthened using EBR and EBROG methods. *Engineering Structures*. 2020; 205: 110072.
- [7] Cristescu MC. Machine learning techniques for improving the performance metrics of functional verification. *Sci. Technol*, 2021; 24(1): 99-116.